high reflectivity coating on the laser back facet. A typical DFB spectrum obtained from the front facet of an integrated MZ/DFB is shown in Fig. 2.

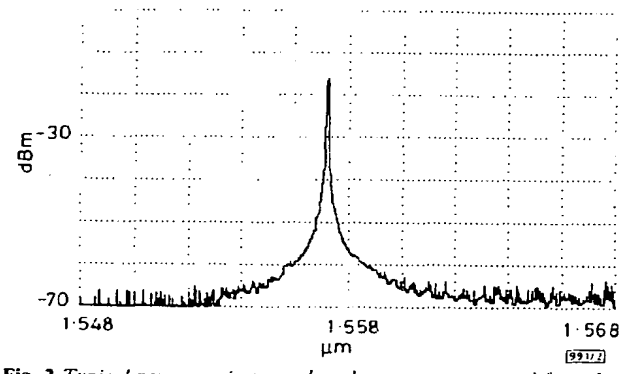


**Fig. 2** *Typical power against wavelength spectrum measured from front facet of integrated MZ/DFB at I = 120mA and T = 20°C*

*Transmission experiment:* The integrated MZ/DFB chip was attached *p*-side-up on an $Al_2O_3$ carrier patterned with coplanar transmission lines terminated with a 50Ω resistor. The DFB was biased at 100mA and the heatsink temperature was set at 20°C. The MZ arms were driven differentially at 10Gbit/s from −4.0 to −2.0V and −3.8 to −5.8V by the output of a pseudorandom bit sequence generator (PRBS). Under these conditions, the extinction ratio was 10.8dB.

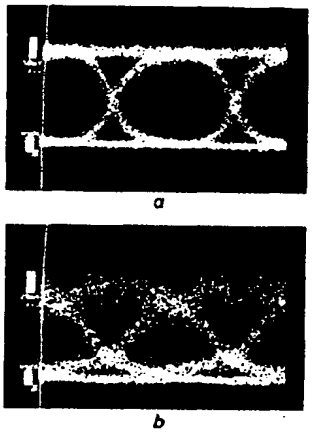


**Fig. 3** *Optical eye diagram at 0km, and after 100km of NDSF*

Horizontal scale is 20ps/div
*a* 0km *b* After 100km

The fibre-coupled MZ/DFB output signal was followed by an optical isolator, an erbium doped fibre amplifier (EDFA), and an optical bandpass filter (1.5nm FWHM) to reduce the amplified spontaneous emission noise from the EDFA. The waveform at 0 km for a PRBS pattern length of $2^7-1$ is shown by the eye diagram in Fig. 3*a*. The eye diagram obtained by a Tektronix SD-46 photodetector after 100km of NDSF is given in Fig. 3*b*. An optical receiver based on an SAGCM APD [8] with an HBT preamplifier (500Ω transimpedance) was employed to assess the dispersion penalty after transmission through 100km of NDSF. The BER against received power curves at 0 and 100km both obeyed a classic logarithmic waterfall form, with no evidence of BER flooring. The displacement between the two BER curves revealed a penalty of only 0.8dB, which is in reasonable agreement with the performance of a discrete III-V MZ device [9].

*Conclusion:* An InGaAsP/InP MZ modulator integrated by butt-coupling with a gain-coupled distributed-feedback laser has been demonstrated for the first time. 10Gbit/s transmission over 100km of NDSF at λ = 1.55μm is achieved with a receiver penalty of <1dB. Approximately 90% of the integrated gain-coupled DFBs lase in a single longitudinal mode at 100mA.

*Acknowledgments:* The authors would like to thank B. Richardson, M. Cleroux, T. Jones, J. Marks and Z. Husain for their technical assistance.


*10 January 1996*
*Electronics Letters Online No: 19960324*

D.M. Adams, C. Rolland, N. Puetz, R.S. Moore, F.R. Shepherd, H.B. Kim and S. Bradshaw (*Bell-Northern Research Ltd., Box 3511, Station C, Ottawa, K1Y 4H7, Canada*)

## References

1 CARTLEDGE, J.C., ROLLAND, C.R., LEMERLE, S., and SOLHEIM, A.: 'Theoretical performance of 10Gb/s lightwave systems using a III-V semiconductor Mach-Zehnder modulator', *IEEE Photonics Technol. Lett.*, 1994, **6**, pp. 282–284

2 ZUCKER, J.E., JONES, K.L., NEWKIRK, M.A., GNALL, R.P., MILLER, B.I., YOUND, M.G., KOREN, U., BURRUS, C.A., and TELL, B.: 'Quantum-well interferometric modulator monolithically integrated with 1.55mm tunable distributed Bragg reflector laser', *Electron. Lett.*, 1992, **28**, pp. 1888–1889

3 TANBUN-EK, P.F., SCIORTINO, P.F., SERGENT, A.M., WECHT, K.W., WISK, P., CHEN, Y.K., BETHEA, C.G., and SPUTZ, S.K.: 'DFB lasers integrated with Mach-Zehnder optical modulator fabricated by selective area growth, MOVPE technique', *IEEE Photonics Technol. Lett.*, 1995, **7**, pp. 1019–1021

4 ROLLAND, C., MOORE, R.S., SHEPHERD, F., and HILLIER, G.: '10Gbit/s 1.56μm multiquantum-well InP/InGaAsP Mach-Zehnder optical modulator', *Electron. Lett.*, 1993, **29**, pp. 471–472

5 ADAMS, D.M., and MAKINO, T.: 'Mechanism for enhanced gain periodicity for truncated-well gain-coupled DFB lasers', *Electron. Lett.*, 1995, **31**, pp. 976–977

6 LU, H., BLAAUW, C., and MAKINO, T.: 'High temperature single-mode operation of 1.3mm strained MQW gain-coupled DFB lasers', *IEEE Photonics Technol. Lett.*, 1995, **7**, pp. 611–613

7 LI, G.-P., MAKINO, T., LU, H., HONG, J., and HUANG, W.: 'External feedback sensitivity of 1.55μm gain-coupled multi-quantum-well DFB lasers', Proc. SPIE, Laser Diode Tech. Appl. VI, 1994, **2148**, pp. 238–245

8 TAROF, L.E., BRUCE, R., KNIGHT, D.G., YU, J., KIM, H.B., and BAIRD, T.: 'Planar InP-InGaAs single growth avalanche photodiodes with no guard rings', *IEEE Photonics Technol. Lett.*, 1995, **7**, pp. 1330–1332

9 ROLLAND, C.R., O'SULLIVAN, M.S., KIM, H.B., MOORE, R.S., and HILLIER, G.: '', OFC'93, San Diego, CA, 1993, Paper PD 27

# Stimulated emission from current injected InGaN/AlGaN surface emitting diode with Al reflector at room temperature

T. Egawa, Y. Murata, T. Jimbo and M. Umeno

*Indexing terms: Light emitting diodes, Stimulated emission*

The authors report the first observation of stimulated emission from a pulsed current injected InGaN/AlGaN surface emitting diode with Al reflectors at room temperature. The InGaN/AlGaN surface emitting diode, which consists of Al reflectors as top and bottom mirrors, was grown on a sapphire substrate using metalorganic chemical vapour deposition. The emission at 380nm exhibited a spectral narrowing, a superlinear dependence of output intensity on injected current, and a shift of the peak emission towards longer wavelengths under a pulsed condition at room temperature.

GaN-based wide-band-gap materials have received much attention for both optical and electronic applications [1]. The interest in GaN-based optical devices has grown dramatically with the recent development of high-efficiency blue LEDs [2]. Recent study has been focussed on the development of the laser diode [3, 4]. However, it is difficult to make facet mirrors by cleaving because this material is very hard. In this study, we observe room-temperature stimulated emission from a pulsed current injected InGaN/AlGaN surface emitting diode with Al reflectors.

The sample in this study was grown on a sapphire substrate with (0001) orientation (c face) using metalorganic chemical vapour deposition (MOCVD) at atmospheric pressure using a modified two step growth technique. Trimethylgallium (TMG), trimethylaluminium (TMA), trimethylindium (TMI), monosilane ($SiH_4$), bis-cyclopentadienyl magnesium ($Cp_2Mg$), diethylzinc (DEZn) and ammonia ($NH_3$) were used as Ga, Al, In, Si, Mg, Zn and N sources, respectively. At first, the substrate was heated to 1050°C in a hydrogen ambient to remove the oxide. Then, the substrate temperature was lowered to 500°C to grow a 25nm thick GaN buffer layer. After that, the device structure was grown as shown in Fig. 1. The device layers consist of a 4mm thick Si-doped *n*-GaN layer at 1020°C, a 150nm thick Si-doped *n*-$Al_{0.15}Ga_{0.85}N$ layer at 1020°C, a 50nm thick Si and Zn codoped

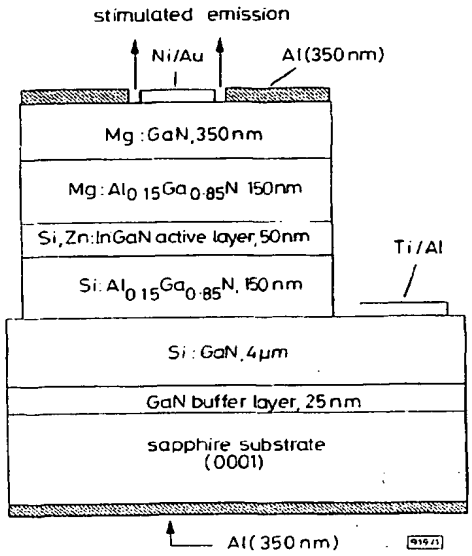


**Fig. 1** *Cross-sectional structure of InGaN/AlGaN surface emitting diode with Al reflectors*

$In_{0.06}Ga_{0.94}N$ layer at 780°C, a 150nm thick Mg-doped $Al_{0.15}Ga_{0.85}N$ layer at 1020°C, and a 350nm thick Mg-doped *p*-type GaN cap layer at 1020°C. After the growth, the sample was partially etched until the *n*-GaN layer was exposed. The ohmic electrodes of Ni/Au and Ti/Al were formed using vacuum evaporation on the *p*- and *n*-GaN layers, respectively. To fabricate the mirror,

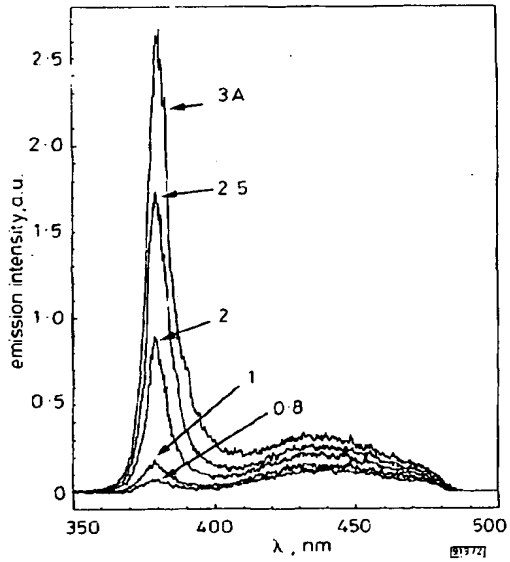


**Fig. 2** *Surface emitting spectra measured at various injected currents*

InGaN/AlGaN surface emitting diode with Al reflector
300K
Pulsed, 0.1μs, 1kHz

350nm thick Al was evaporated onto the surface and the back of the sample. The measured reflectivity was ~90%. The spectra from the surface were measured using an optical multi-channel analyser (Seiko EG&G, OMA IV) under the pulsed condition (0.1μs, 1kHz) at room temperature.

Fig. 2 shows the surface emitting spectra measured at the various injected pulsed currents. For the injected currents below 0.3A, the broad spontaneous emission was observed at ~437nm with the full width at half-maximum (FWHM) of 63nm. The emission at 437nm arises from the impurity related emission in the InGaN active layer [5]. As the injected current increases, the emission intensity of 437nm increases and a new emission feature with a much narrower line shape appears at 380nm. When the injected current increases further, the emission at 380nm becomes strong-

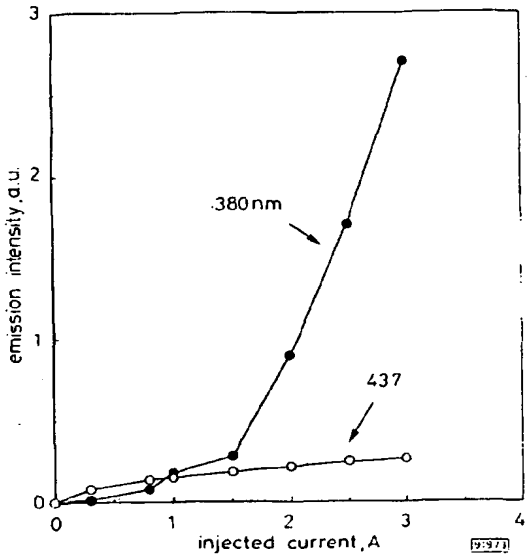


**Fig. 3** *Dependence of surface emitting spectrum peak intensity on injected current for 380 and 437nm emissions*

InGaN/AlGaN surface emitting diode with Al reflector
300K
Pulsed, 0.1μs, 1kHz

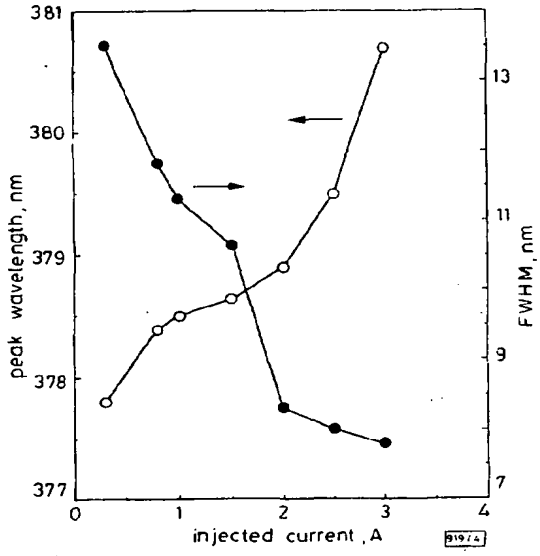


**Fig. 4** *Peak wavelength and its FWHM against injected current*

300K
Pulsed, 0.1μs, 1kHz

and sharp above the injected current of 2A. The emission at 380nm originates from band-to-band emission in the InGaN active layer. Fig. 3 shows the dependence of the surface emitting

spectrum peak intensity on the injected current for these two mode emissions. The intensity of 437nm emission increased gradually and had a tendency to saturation as the injected current was increased. This is caused by the saturation of the impurity recombination centres in the InGaN active layer. As the injected current increases, conversely, the intensity of 380nm emission increases rapidly above the threshold injected current of 1.5A. The threshold for stimulated emission is estimated to be ~10kA/cm$^2$. The 380nm emission exhibited superlinear dependence on the injected current, indicating the onset of stimulated emission.

To further confirm the presence of stimulated emission we show the peak wavelength and its FWHM against injected current in Fig. 4. A clear spectral narrowing and its shift to longer wavelength were observed by increasing the injected current. The peak wavelength shifted to a longer wavelength, from 377.8nm at 0.3A to 380.7nm at 3A. The FWHM narrowed from 13.5nm at 0.3A to 7.8nm at 3A. Thus, spectral narrowing, superlinear dependence of output intensity on injected current, red shift and sharp threshold were clearly observed in the InGaN/AlGaN surface emitting diode with the Al reflectors. To compare the characteristic of the surface emitting diode with and without the Al reflectors, we also measured the dependence of peak intensity of the injected current for the conventional LED without the Al reflectors. The conventional LED without the Al reflectors showed linear light output-injected current characteristic. A superlinear increase of light output power and a spectral narrowing were not observed in this structure.

We have achieved room-temperature stimulated emission from the current injected InGaN/AlGaN surface emitting diode with Al reflectors grown on the sapphire substrate by MOCVD technique for the first time. Room-temperature stimulated emission was evidenced by spectral narrowing, superlinear dependence of output intensity on injected current, red shift and sharp threshold in the InGaN/AlGaN surface emitting diode with the Al reflectors.


*4 January 1996*
*Electronics Letters Online No: 19960291*

T. Egawa, T. Jimbo and M. Umeno (*Research Center for Micro-Structure Devices, Nagoya Institute of Technology, Gokiso-cho, Showa-ku, Nagoya 466, Japan*)

Y. Murata (*Department of Electrical and Computer Engineering, Nagoya Institute of Technology, Gokiso-cho, Showa-ku, Nagoya 466, Japan*)

## References

1 MORKOC, M., STRITE, S., GAO, G.B., LIN, M.E., SVERDLOV, B., and BURNS, M.: 'Large-band-gap SiC, III-V nitride, and II-VI ZnSe-based semiconductor device technologies', *J. Appl. Phys.*, 1994, **76**, pp. 1363–1398

2 NAKAMURA, S., SENOH, M., and MUKAI, T.: 'High-power InGaN/GaN double-heterostructure violet light emitting diodes', *Appl. Phys. Lett.*, 1993, **62**, pp. 2390–2392

3 EGAWA, T., MURATA, Y., JIMBO, T., and UMENO, M.: 'First observation of stimulated emission from current injected InGaN/AlGaN double-heterostructure diode'. Int. Electron Devices Meeting Tech. Dig., Washington DC, 1995, pp. 1005–1006

4 AKASAKI, I., AMANO, H., SOTA, S., SAKAI, H., TANAKA, T., and KOIKE, M.: 'Stimulated emission by current injection from an AlGaN/GaN/GaInN quantum well device', *Jpn. J. Appl. Phys.*, 1995, **34**, pp. L1517–L1519

5 NAKAMURA, S., MUKAI, T., and SENOH, M.: 'High-brightness InGaN/AlGaN double-heterostructure blue-green-light-emitting diodes', *J. Appl. Phys.*, 1994, **76**, pp. 8189–8191

# Attenuation and cross-polarisation caused by trees at millimetre wavelengths

I.J. Dilworth

*Indexing term: Radiowave propagation*

Measurements of forward attenuation at 38GHz caused by tree branches and leaves are reported. Co-polarised and cross-polarised characteristics from several European trees when wet and dry, both with and without foliage, are presented. These data will find practical application in the systems design of proposed multipoint video distributions systems (MVDS) and in the general area of the operation of millimetre wave links e.g. PCN.

*Introduction:* The increasing use of millimetre wave links for point to point communications, e.g. the so called private communications network (PCN) and the proposed introduction of point to multipoint millimetre wave broadcasting of video (MVDS) require good workable systems planning tools to be available. Few measurements of attenuation and cross-polarisation at millimetre wavelengths have been reported [1, 6] yet the effects of partial or total obscuration of the Fresnel zones of millimetre wave paths by deciduous and non deciduous tree foliage and by tree branches are of practical interest.

For example, path lengths for millimetre wave links and the proposed MVDS are relatively short, up to ~1km. It is quite practical, in most cases, to avoid obscuration of the first Fresnel zone, especially for MVDS installations, which will typically be from domestic rooftops to local 'transmitter nodes' mounted on lamp posts. However, often the path will pass near to, or suffer actual obscuration by, a tree. Trees grow and paths may become obscured so it is of practical interest to find out whether millimetre wavelengths suffer serious attenuation and cross-polarisation in such circumstances, and indeed whether PCN and MVDS will be practical if a few metres of foliage is present in the first Fresnel zone region. Empirical and semi-empirical models do exist for predicting the attenuation from foliage e.g. [6] but these models concentrate on propagation through relatively large vegetation depths to predict shielding values. No cross-polarisation measurements have so far been reported. Theoretical modelling of foliage attenuation has been attempted [2] but models are limited to frequencies below ~14GHz so far.

Here we report on millimetre wavelength attenuation and cross-polarisation measurements made on several types of tree, both when the tree leaves were wet and when they were dry. These measurements were repeated when the trees were with and without leaves i.e. in the summer and winter.

*Experimental method:* To have a representative selection of leaf sizes Ash, Oak, Sycamore, Silver Birch and (evergreen) Llandii species were used in the tests. The experimental method and the equipment used have been described, together with alignment and measurement error issues, [1] and these details will not be repeated in this Letter. The antennas were operated well into their far field region and the diameter of the first Fresnel zones, at the trees, was 1–3m. The number of branches and leaves in each common volume was estimated and in each case the branches and leaves exceeded a hundred. The illuminating field was vertically polarised and the antennas consisted of three identical, commercially produced, biconvex lens horns. The cross-polar measurements reported here are limited by the poor antenna characteristics [3] which, at its maximum co-polar response (boresight) results in a cross-polar discrimination of ~24dB. Since this is a commercial antenna it would appear that good cross-polar performance is difficult to achieve economically at these millimetre wavelengths. Interference protection (or frequency re-use) by means of orthogonal polarisations will be affected by cross-polarisation generated by foliage and branches. The results are, at the current time, representative or perhaps better than those which may practically be experienced in a MVDS/PCN link since great care was taken in antenna alignment, which is unlikely to be practical in planning the antennas in a commercial PCN installation.